Neuron, Vol. 30, 227–240, April, 2001, Copyright ©2001 by Cell Press

Selective Targeting of Newly Synthesized *Arc* mRNA to Active Synapses Requires NMDA Receptor Activation

Oswald Steward*‡ and Paul F. Worley†
*Reeve-Irvine Research Center and
Department of Anatomy and Neurobiology and
Department of Neurobiology and Behavior
College of Medicine
University of California at Irvine
Irvine, California 92697
†Department of Neuroscience
Johns Hopkins University School of Medicine
Baltimore, Maryland 21205

Summary

Newly synthesized *Arc* mRNA is selectively targeted to synapses that have experienced particular patterns of activity. Here, we demonstrate that the targeting requires NMDA receptor activation. *Arc* expression was induced by an electroconvulsive seizure, and the newly synthesized mRNA was then targeted to synaptic sites by activating the perforant path projections to the dentate gyrus. When micropipette electrodes containing NMDA receptor antagonists (MK801 or APV) were positioned in the dentate gyrus during the stimulation period, newly synthesized *Arc* mRNA was transported into dendrites but did not localize in the activated lamina; instead, the mRNA remained diffusely distributed. AMPA receptor antagonists (CNQX) blocked targeting of *Arc* mRNA in a small region, and mGluR antagonists (MCPG) did not affect localization. These results demonstrate that NMDA receptor activation is required for the targeting of *Arc* mRNA to active synapses.

Introduction

Strong synaptic activation of cortical neurons induces the expression of a number of immediate early genes (IEGs). Of the IEG mRNAs that are induced in this fashion, *Arc* (activity-regulated cytoskeleton-associated protein), also known as *Arg 3.1*, is so far unique because its mRNA is rapidly delivered into dendrites (Link et al., 1995; Lyford et al., 1995).

An especially interesting feature of *Arc* is that newly synthesized *Arc* mRNA accumulates selectively near synaptic sites that have experienced strong activity. For example, activation of the perforant path projection to the hippocampal dentate gyrus using stimulation patterns that induce LTP causes *Arc* mRNA to localize selectively in the dendritic segments that receive perforant path synapses (Steward et al., 1998). This targeting of newly synthesized mRNA to active synapses represents a novel mechanism for synapse-specific delivery of gene products induced by the synaptic activation. This mechanism is well suited to play a role in the forms of activity-dependent synaptic modification that require protein synthesis (Frey and Morris, 1997; Kang and Schumann, 1996; Martin et al., 1997; Nguyen and Kandel, 1996).

Given the potential role that mRNA targeting could play in synaptic modifications that require gene expression, it is important to define the signal transduction mechanisms that mediate the synaptic localization. One issue is whether the localization requires the activation of particular types of neurotransmitter receptors, or on the local depolarization and/or resulting ionic flux produced by the synaptic activation. The present study addresses this question, focusing on the example of *Arc* mRNA localization that occurs after patterned stimulation of the projections from the medial entorhinal cortex to the dentate gyrus (the medial perforant path). The perforant path is glutamatergic, and transmission at these synapses involves ionotropic receptors (AMPA and NMDA) and metabotropic receptors (mGluR).

If localization requires the activation of particular receptors, then the localization process ought to be disrupted by selective pharmacological blockade of the particular receptor type. To assess the role of the different receptors in mediating mRNA localization, micropipette-recording electrodes filled with receptor antagonists were positioned in the dentate gyrus during the stimulation period. The antagonists diffuse from the micropipettes, creating a region in which the action of the particular receptor is blocked. Areas distant from the micropipette serve as an internal control.

Using a paradigm in which *Arc* mRNA is induced by a generalized stimulus (an electroconvulsive seizure, ECS), and subsequently targeted to particular dendritic domains by synaptic activation, we demonstrate that activation of NMDA receptors during afferent activation is required for targeting *Arc* mRNA to active synapses.

Results

We have previously shown that high frequency stimulation of the medial perforant path induces *Arc* expression in the dentate gyrus and causes the newly synthesized mRNA to localize selectively in the middle molecular layer—exactly the region in which the perforant path terminates (Steward et al., 1998). To study the signals that mediate this targeting, it is important to differentiate between the signals that induce *Arc* expression and those that mediate the localization. To this end, we used a paradigm in which *Arc* expression is induced by delivering an electroconvulsive seizure (ECS), and then the newly synthesized mRNA is targeted to particular dendritic domains by subsequent synaptic activation.

The paradigm was as follows. An ECS was induced in an unanesthetized rat to induce *Arc* expression bilaterally. Then, the rat was anesthetized, and stimulation and recording electrodes were positioned so as to activate the medial perforant path on one side. The time between the ECS and the completion of the preparation for physiology was typically 30–45 min. Baseline response amplitude was assessed using stimuli that initially evoked an approximately half-maximal population

‡To whom correspondence should be addressed (e-mail: osteward@uci.edu).

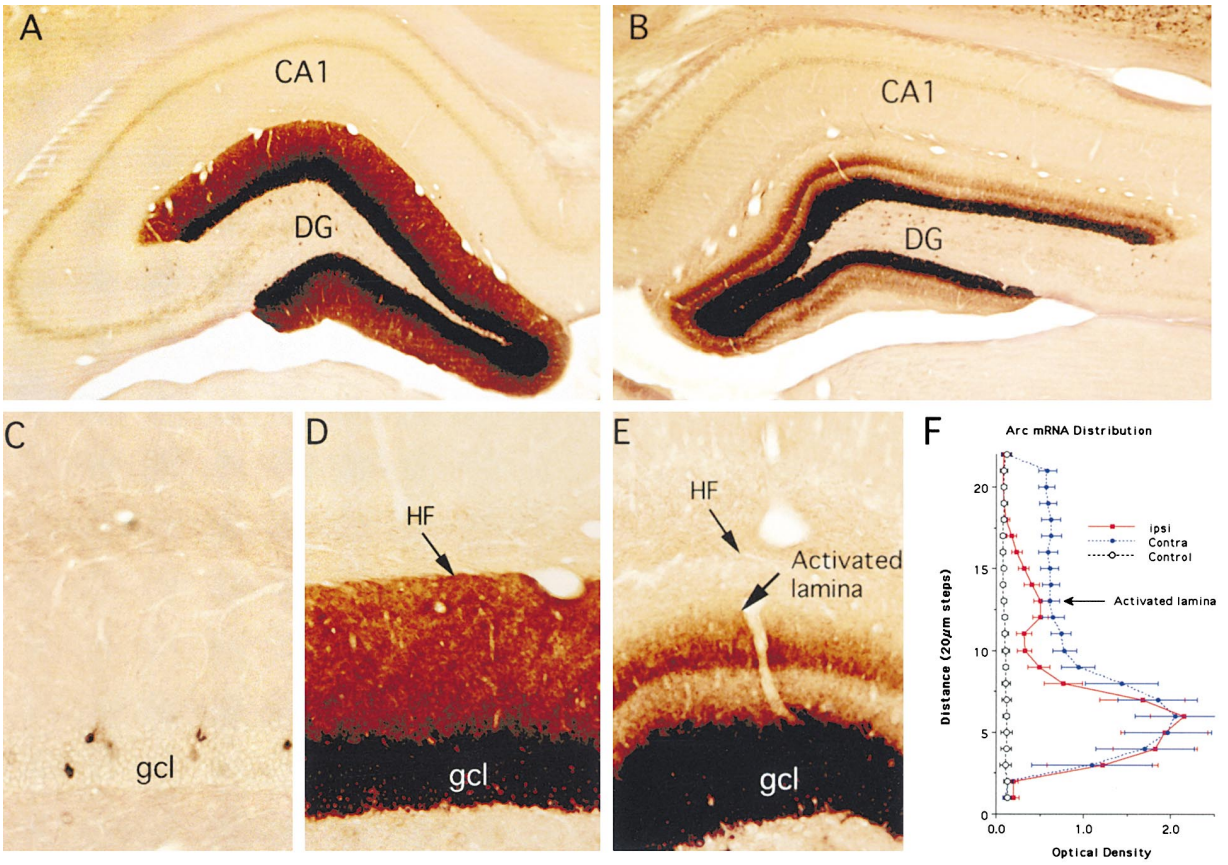

Figure 1. Selective Targeting of Arc mRNA to Active Dendritic Domains after Induction by Electroconvulsive Seizures

The photomicrographs illustrate the distribution of *Arc* mRNA as revealed by nonisotopic in situ hybridization. In this experiment, a single ECS was delivered to induce *Arc* expression bilaterally. Then, the rat was anesthetized, and stimulation and recording electrodes were positioned so as to activate the medial perforant path on the right side. The perforant path was then stimulated at high frequency for 2 hr.

(A) Distribution of *Arc* mRNA on the side contralateral to the stimulation where *Arc* expression had been induced by the ECS. Note that *Arc* mRNA is distributed uniformly across the molecular layer.

(B) Distribution of *Arc* mRNA on the side that had received perforant path stimulation. Note the discrete band of labeling in the middle molecular layer of the dentate gyrus (the site of termination of projections from the medial perforant path).

(C) Distribution of *Arc* mRNA in the dentate gyrus of control animals.

(D) High power view of the distribution of *Arc* mRNA in the dentate gyrus contralateral to the stimulation where *Arc* expression had been induced by the ECS (from A).

(E) High power view of the distribution of *Arc* mRNA in the dentate gyrus that had received perforant path stimulation (from B).

(F) Graph illustrating the average optical density (OD) of labeling across the molecular layer from the cases illustrated in C (control), D (contra), and E (ipsi). Bars indicate the standard deviation of the five measurements at each level.

CA1 field of the hippocampus (CA1), dentate gyrus (DG), granule cell layer (gcl).

spike (3–5 mV amplitude); then high frequency trains (400 Hz trains, eight pulses per train) were delivered at a rate of 1/10 s. Initially, three bouts of ten trains were given, and between each bout, ten single test pulses were delivered to monitor synaptic potentiation. Interestingly, the high frequency stimulation consistently produced robust synaptic potentiation, despite the fact that an ECS had previously been induced. After documenting the degree of synaptic potentiation, trains were delivered at a rate of 1/10 s for various time periods.

The pattern of *Arc* mRNA localization following this ECS/perforant path stimulation paradigm is illustrated in Figure 1. In this experiment, stimulation was delivered for 2 hr, as the *Arc* mRNA that had been induced by the ECS was migrating into the dendrites. As expected, *Arc* mRNA was strongly induced in the dentate gyrus on both sides (compare Figure 1C, which illustrates the distribution of *Arc* mRNA in a nonstimulated animal, with Figures 1D and 1E). On the side contralateral to the perforant path stimulation, the *Arc* mRNA that had been induced by the ECS was diffusely distributed throughout the dendritic lamina (Figures 1A and 1D). In contrast, on the stimulated side, *Arc* mRNA was localized in a discrete band in the middle molecular layer corresponding to the zone of termination of the activated synapses (Figures 1B and 1E). Hence, *Arc* mRNA that would otherwise have been distributed diffusely in the dendrites following the ECS became highly localized in the activated dendritic domain as a consequence of synaptic stimulation.

Quantitative assessment of the distribution of *Arc* mRNA across the molecular layer revealed that the dis-

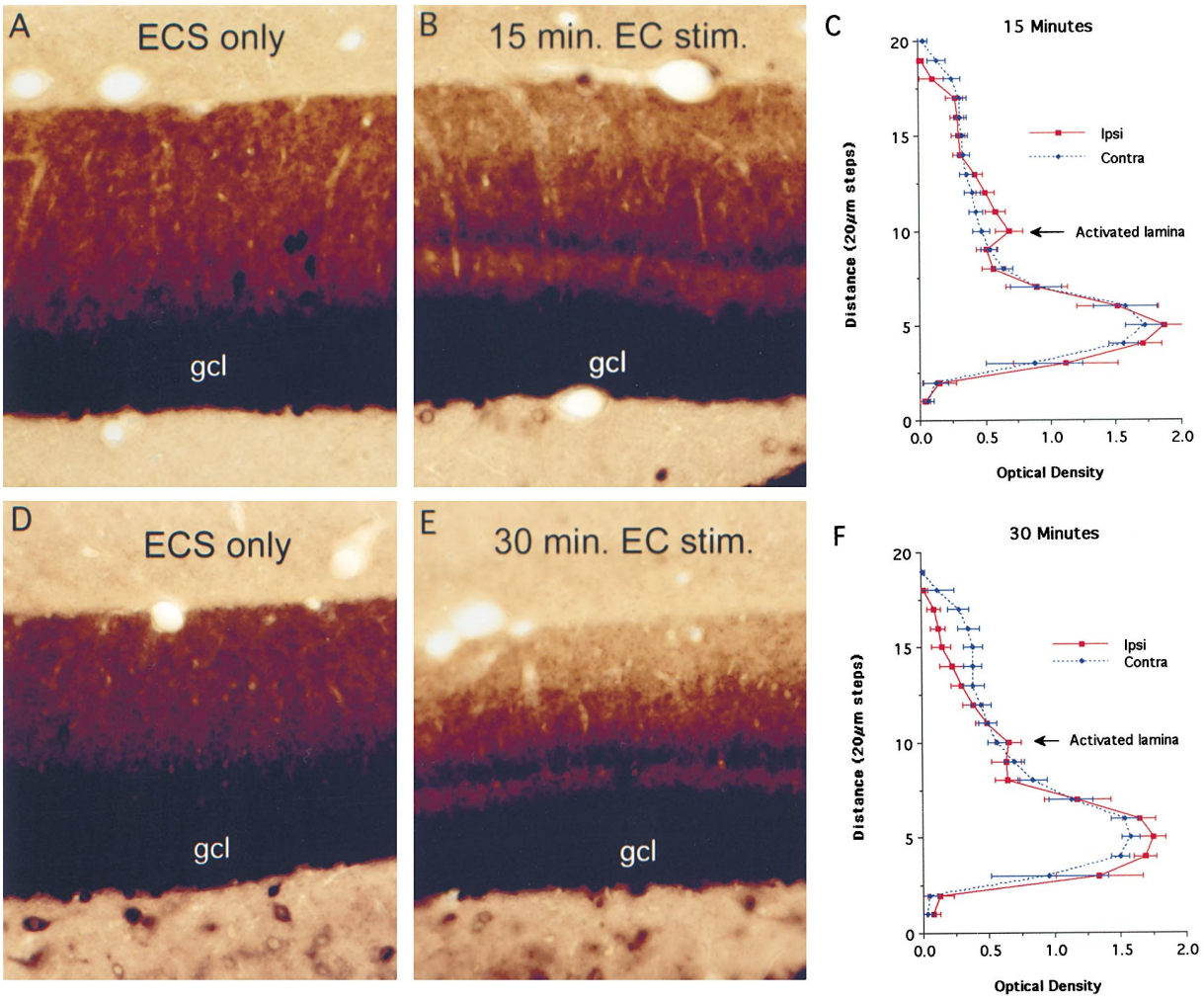

Figure 2. Dynamics of mRNA Targeting to Activated Dendritic Domains

To define the dynamics of the redistribution of newly synthesized *Arc* mRNA within dendrites, rats received an ECS, and then high frequency trains were delivered to the perforant path for a 15 (A and B), or 30 (D and E) min period just before the animals were euthanized and perfused for in situ hybridization.

(A and D) Pattern of labeling on the side contralateral to the stimulation where Arc had been induced by the ECS only.

(B and E) Pattern of labeling on the side of the stimulation.

(C and F) The graphs illustrate the optical density (OD) across the molecular layer in the areas illustrated. Abbreviations are as in Figure 1.

tinctness of the band was due in part to the fact that levels of labeling were lower in the nonactivated dendritic laminae on the stimulated side than on the side that had experienced the ECS only. For example, levels of labeling were near background in the outer molecular layer, which contains the dendritic segments distal to the site of termination of the activated synapses. Levels of labeling were also lower in the inner molecular layer, which contains the proximal dendrites through which the mRNA would have to move to reach the middle dendritic zones (see Figure 2E). There are two possible explanations of the lower levels of labeling in nonactivated laminae: (1) the newly synthesized mRNA quickly passes through the proximal dendrites and then docks selectively in the middle dendrites, never reaching distal segments or (2) synaptic activation causes an overall increase in mRNA degradation in dendrites but stabilizes the mRNA in the activated domain.

Dynamics of mRNA Targeting to Activated Dendritic Domains

In the above paradigm, synaptic stimulation began about 30–45 min after the ECS (the time it took to anesthetize the animal and place electrodes for acute neurophysiology). Thus, the 2 hr of stimulation would be taking place as the *Arc* mRNA that had been induced by the ECS was migrating into the dendrites. To further elucidate how synapse-specific localization occurred, we evaluated how synaptic activity affected mRNA distribution when the mRNA was already distributed throughout the dendrites.

For this experiment, rats received an ECS, and then high frequency trains were delivered to the perforant path beginning 1.5 or 1.75 hr after the ECS. Stimulation was then delivered for the 30 or 15 min period respectively just before the animals were euthanized and perfused for in situ hybridization (in both cases, perfusion

occurred 2 hr after the ECS). It is important to note that at 1.5 or 1.75 hr post ECS, *Arc* mRNA would have been present in the dendrites when the stimulation was initiated. Remarkably, 15 min of synaptic stimulation was sufficient to produce a prominent band of labeling for *Arc* mRNA in the middle molecular layer of the dentate gyrus (Figure 2B). Levels of labeling were higher in this band than on the opposite side, which had received an ECS only (compare Figures 2A and 2B, and for quantification, see Figure 2C). Because the band developed so quickly, the accumulation is likely to represent redistribution of the *Arc* mRNA that is already in the dendrite rather than transport of *Arc* mRNA from the cell body.

Following 30 min of stimulation, the band became more distinct as levels of labeling decreased in the nonactivated laminae, especially in the outer molecular layer (Figures 2E and 2F). These results indicate that synaptic activation both causes newly synthesized *Arc* mRNA to rapidly redistribute to the activated zone (as is evident with 15 min of stimulation) and also depletes the mRNA from nonactivated regions of the dendrites (as seen with 30 min or more of stimulation).

It is noteworthy that after prolonged periods of synaptic stimulation (2 hr), the overall levels of labeling in the molecular layer are lower than on the side that received an ECS only (Figure 1). This suggests that in addition to causing the newly synthesized mRNA to redistribute to active synaptic sites, synaptic activation may also enhance mRNA degradation. This enhanced degradation could be linked to the targeting of the mRNA to the activated zone or could be due to signals generated throughout the dendrite as a consequence of the intense depolarization (more on this below).

Physiological Documentation of GluR Antagonist Action

To define the signals that cause *Arc* mRNA to localize at active synapses, micropipettes containing glutamate receptor antagonists were positioned in the dentate gyrus during high frequency stimulation. It was first necessary, however, to document the effects of GluR antagonists on synaptic responses; this was done in animals that had *not* received a prior ECS.

To characterize the physiological consequences of having GluR antagonists in the micropipette recording electrodes, a saline-filled electrode was first positioned in the molecular layer of the dentate gyrus so as to record the negative-going population EPSP (for sample traces, see Figure 3). Baseline responses were recorded, and then the saline-filled micropipette was removed and replaced with a micropipette filled with saline or with a particular antagonist, taking care to reposition the electrode precisely in the middle molecular layer of the dentate gyrus where the negative-going population EPSP was at its maximum. Single-pulse stimulation was then delivered to assess response amplitude, and then three bouts of high frequency stimulation (ten trains of eight pulses at 400 Hz) were delivered. Between each bout, ten test pulses were collected to assess the degree of synaptic potentiation.

In control experiments, the microelectrode was removed and replaced by another filled with saline. Following these exchanges, response amplitude usually decreased transiently, and then recovered within about 5 min to a level that was near the preexchange baseline (Figure 3A). In six such control electrode exchanges, the average change in response amplitude after recovery was 7% $\pm$ 18% (Figure 3D).

AMPA Receptor Antagonists

When a saline-filled electrode was replaced by one filled with CNQX or DNQX, the amplitude of the negative-going population EPSP began to decrease within seconds after the electrode was positioned, and was not detectable within a few minutes. Figure 3B illustrates a representative experiment involving CNQX. Because the results with the two AMPA receptor antagonists were very similar, we illustrate results only for experiments involving CNQX. As the negative-going response disappeared, a small positive-going response remained; this likely reflects a volume-conducted response from distant sites. Because of the small residual positive response, the average change in response amplitude in six experiments was $-111\% \pm 9\%$ (Figure 3D).

One technical aside: In experiments in which the micropipette was positioned in the cell body layer so as to record the positive-going EPSP, response amplitude was reduced by 80%–90% by AMPA receptor antagonists, but a small positive response could still be recorded. The small residual response in the presence of CNQX or DNQX probably reflects a volume-conducted response from distant sites rather than reflecting incomplete blockade of synaptic transmission. This interpretation is supported by the fact that the negative-going EPSP in the molecular layer was blocked, so that the characteristic reversal of the response was not seen as the microelectrode was moved through the dentate gyrus (data not shown). This is indicative of a volume-conducted response that is generated by synaptic currents at a distant site.

NMDA Receptor Antagonists

When a saline micropipette was replaced with one filled with MK801 or APV, EPSP slope recovered to near the preexchange baseline (Figures 3C and 3D). In six experiments involving MK801, the average change in EPSP slope was 3% $\pm$ 19%; in eight experiments involving APV, the average change in EPSP slope was 5% $\pm$ 28% (see Figure 3F). The lack of effect on population EPSP slope is consistent with the fact that NMDA receptors play a minimal role in the fast EPSP generated by single pulse stimulation.

Although NMDA antagonists did not affect baseline synaptic responses generated by single pulse stimulation, NMDA antagonists had two other prominent effects. First, they blocked the late negativity generated by high-frequency stimulation (Figure 4A). Second, they blocked the synaptic potentiation that would otherwise be induced by high-frequency stimulation. Figures 4B–4D illustrate data from experiments in which either MK801 or APV was present in the recording micropipette. The graphs plot the average slope of the last 30 responses prior to high-frequency stimulation, and the ten test responses after each of three bouts of ten 400 Hz trains. In control experiments ($n = 5$), EPSP slope increased by an average of 63% $\pm$ 6.4%; in contrast, when either MK801 or APV was present in the recording micropipette, synaptic potentiation was blocked. The bar graph in Figure 4D illustrates the mean changes in

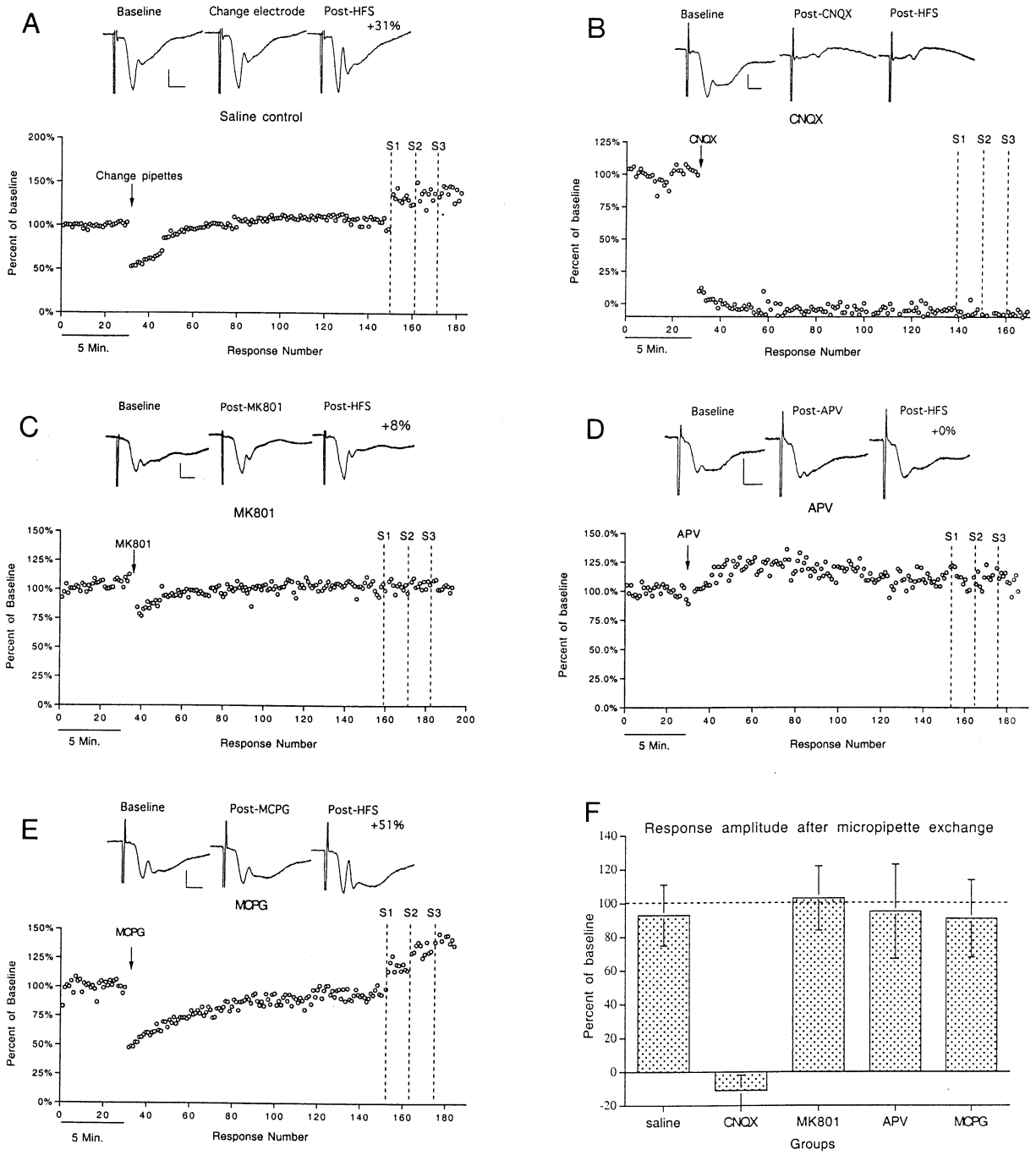

Figure 3. Differential Effects of GluR Antagonists on Synaptic Transmission

To document the efficacy of GluR antagonists, a saline-filled electrode was first positioned in the dentate gyrus so as to record the negative-going population EPSP generated by perforant path stimulation. This electrode was then removed and replaced with a micropipette filled with either saline or various GluR antagonists. The exchange generally required 2–3 min, and thus the time-base of the graph is broken at the time of electrode exchange (marked by the arrow).

(A) An example of an experiment in which a saline-filled micropipette was replaced with another filled with saline. Note the transient decrease in population EPSP amplitude followed by a recovery to near baseline. The traces illustrate sample responses during the baseline period, at the end of the test period following micropipette exchange, and after three bouts of high-frequency stimulation (HFS).

(B) An experiment in which the saline micropipette was exchanged for a micropipette filled with CNQX. Note the rapid disappearance of the EPSP.

(C–E) Experiments in which the saline micropipette was exchanged for a micropipette filled with MK801 (C), APV (D), and MCPG (E). Note the recovery of the response after micropipette exchange to near baseline levels. After collecting test responses for 20 min, three bouts of high frequency stimulation (S1, S2, and S3) were delivered to induce LTP. The right-hand traces in each panel illustrate responses after the delivery of the high frequency stimulation (post-HFS). Note the blockade of LTP in the experiments involving MK801 and APV.

(F) The bar graph illustrates the average change in response amplitude after electrode exchange in the different experiments.

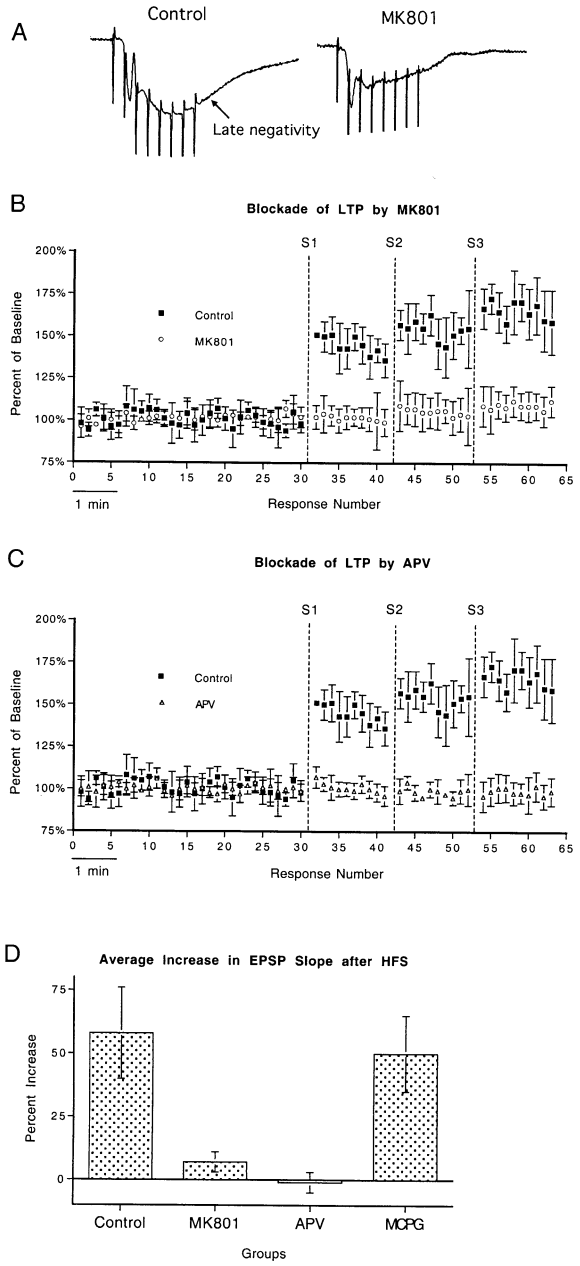

Figure 4. Blockade of LTP Induction by MK801

(A) Sample evoked responses generated by high-frequency stimulation recorded via a saline-filled micropipette (control) or a micropipette filled with MK801. Note the slow negativity in the control, which is blocked by MK801. Similar results were obtained with APV-filled micropipettes.

(B) The graphs plot the average slope of the last 30 responses prior to high frequency stimulation, and the ten test responses after each bout of ten 400 Hz trains in five representative control experiments and six experiments in which MK801 was present in the recording micropipette.

(C) The graph illustrates the comparison between the same five control experiments and eight experiments in which APV was present in the micropipette.

(D) The bar graph illustrates the average change in EPSP slope after HFS in the different groups. Note the blockade of LTP by MK801 and APV, whereas MCPG does not affect the induction of LTP.

response amplitude after three bouts of high frequency stimulation. In six experiments involving MK801, the mean change in EPSP slope was +7% ± 4%; in eight experiments involving APV, the mean change in EPSP slope was +1% ± 3.7%.

It should be noted the late negativity in response to high-frequency stimulation was also blocked by CNQX (data not shown). This indicates that in the presence of an AMPA receptor antagonist, there was also minimal current flow through the NMDA receptor. This is consistent with the fact that current flow through the NMDA receptor occurs only when the cell is sufficiently depolarized, which can occur either by AMPA receptor coactivation or by action potential back propagation.

MGluR Receptor Antagonists

When a saline micropipette was replaced by one filled with MCPG, EPSP slope recovered to near the pre-exchange baseline (Figure 3E). In four experiments, the average change in EPSP slope was 9% ± 23% (Figure 3F). Also, MCPG did not significantly affect the induction of LTP following high frequency stimulation; the average increase in EPSP slope in five experiments in which MCPG was present in the micropipette was 50 ± 15% in comparison to the 63 ± 6.4% in control experiments.

Visualization of the Area of Antagonist Action Using In Situ Hybridization

In situ hybridization analyses of the distribution of *Arc* mRNA yielded striking visual documentation of the area of blockade produced by receptor antagonists. For these experiments, 400 Hz trains were delivered at 1/10 s for 2 hr in order to generate the fully developed localization pattern. MK801 was present in the micropipette during the period of synaptic stimulation; Arc induction was completely blocked in an area about 1 mm in diameter around the micropipette (Figures 5A and 5B). In the area of blockade, labeling was present in a small number of granule cells scattered throughout the granule cell layer in a pattern similar to that seen on the non-stimulated side. At the same time, *Arc* mRNA was strongly induced and selectively localized in the activated lamina in regions distant from the micropipette. When APV was present in the micropipette, the area of blockade was considerably larger (Figure 5C). In the case illustrated, Arc induction was blocked throughout most of the area of the dentate gyrus visible in the section.

In contrast to the large area of blockade produced by NMDA receptor antagonists, the AMPA receptor antagonists blocked Arc induction in a small area (Figure 5D). Again, similar results were obtained with both CNQX and DNQX, so we will illustrate results only for experiments involving CNQX. The case illustrated in Figure 5D is the one in which the area of blockade was largest. In cases treated with mGluR antagonists, there was no detectable effect on Arc induction (Figure 5E).

To provide a quantitative measure of the area of blockade produced by the different antagonists, we measured the linear extent of blockade in the dorsal blade of the dentate gyrus in every other section through a collection of serial sections. The total area of blockade was then reconstructed by stacking the sections at a spacing distance scaled for section thickness (Figure 5F). We then determined the total area of the stack. This value was then averaged across cases (Figure 5G). Measure-

ments were taken only in the dorsal blade because the micropipette tip was positioned in the dorsal molecular layer. In this way, the linear measurements provide an approximate measure of the diameter of the affected area.

This quantitative analysis reveals that APV produced a large area of blockade that extended for several mm rostrocaudally and mediolaterally. MK801 produced a smaller area of blockade that extended for approximately 1 mm away from the micropipette. CNQX produced a very small area of blockade that averaged less than 100 μm in diameter (the case reconstructed in Figure 5F exhibited the largest area of blockade seen in any of the cases). We did not carry out serial reconstructions in cases involving DNQX, but qualitatively, the areas of blockade were similar in size to those produced by CNQX. There was no detectable area of blockade in any of the cases treated with MCPG.

NMDA-Receptor Antagonists Block Targeting of Newly Synthesized *Arc* mRNA to Activated Dendritic Domains

The above results indicate why it is necessary to use an experimental paradigm in which it is possible to dissociate induction from targeting. NMDA antagonists block induction, so it is impossible to study the targeting of the mRNA when it is not synthesized in the first place. Hence, we return to the paradigm in which Arc is induced by an ECS, and then synaptic stimulation is delivered for 2 hr to target newly synthesized Arc mRNA to active synaptic sites (the ECS/EC stimulation paradigm).

When either MK801 or APV was present in the recording micropipette during the stimulation period after an ECS, the selective localization of *Arc* mRNA in the activated zone was completely blocked in the area around the micropipette. Figure 6 illustrates examples of the blockade of localization with MK801 (A) and APV (B). In the areas surrounding the micropipette, the newly synthesized mRNA was distributed uniformly across the molecular layer rather than being localized selectively in the activated lamina. Quantitative analyses of mRNA distribution across the molecular layer (Figures 6D–6F) revealed that NMDA-receptor antagonists blocked the formation of the band of *Arc* mRNA in the activated lamina, and also prevented the stimulation-induced depletion of *Arc* mRNA in nonactivated laminae (the outer and inner molecular layer). Importantly, in areas distant from the micropipette, *Arc* mRNA was still selectively targeted to the activated lamina. This targeting can be seen in the medial most portion of the dentate gyrus in the sections illustrated, and is documented in the plots of OD ("distant site").

The fact that NMDA-receptor antagonists blocked the formation of the band of *Arc* mRNA in the activated lamina and prevented the stimulation-induced depletion of *Arc* has implications for the potential mechanisms underlying the depletion of the mRNA from the inactive laminae. Specifically, in the area of blockade, the high-frequency stimulation still produces strong synaptic depolarization via AMPA receptors, and also massive postsynaptic discharge. Nevertheless, this dendritic depolarization and postsynaptic firing is not sufficient to cause depletion, suggesting that the depletion is not due to a depolarization-induced enhancement of mRNA degradation. Instead, it seems likely that the depletion is coupled with the redistribution of the mRNA to the activated lamina.

In contrast to the pronounced effects of NMDA-receptor antagonists, AMPA-receptor antagonists disrupted localization over a very small area. Figures 6C and 6F illustrate a case involving CNQX, and similar results were obtained with DNQX (data not shown). To compare the areas of blockade produced by the different antagonists, we again reconstructed the total area of blockade through a set of serial sections. As illustrated in the bar graph in Figure 7, both MK801 and APV blocked localization in a large region. In contrast, CNQX blocked localization in a very small region immediately surrounding the micropipette. The sizes of the areas of blockade of localization were generally similar to the sizes of the areas in which induction was blocked in the paradigm involving EC stimulation without prior ECS (compare Figures 5G and 7). Interestingly, however, the band of labeling in the molecular layer was blocked over a somewhat larger area than was the case when measuring the effect of the antagonists on *Arc* induction.

We did not evaluate the effects of mGluR antagonists on activity-dependent localization in the ECS-perforant path stimulation paradigm, because mGluR antagonists did not affect localization in the paradigm involving perforant-path stimulation alone.

Activation of NMDA Receptors Is Sufficient for Induction and Targeting of *Arc* mRNA under Conditions of AMPA-Receptor Blockade

Blockade of fast synaptic transmission by AMPA-receptor antagonists should also block current flow through the NMDA receptor. This is because current flow through the NMDA receptor is blocked by Mg^{2+} unless the cell is sufficiently depolarized. Sufficient depolarization is generated during high frequency stimulation as a result of AMPA-receptor coactivation. Thus, the blockade of induction and targeting produced by CNQX could be due to Mg^{2+} blockade of the NMDA-receptor channel. Nevertheless, we cannot exclude the possibility that AMPA-receptor and NMDA-receptor coactivation is required. To address this question, we developed a novel strategy for activating NMDA receptors under conditions of AMPA-receptor blockade.

The strategy took advantage of the fact that Mg^{2+} blockade of current flow through the NMDA receptor can be relieved by depolarizing the postsynaptic cell. This was accomplished by filling micropipette recording electrodes with 4MKCl rather than 0.9% saline, and then adding CNQX to block AMPA receptors. A representative experiment is illustrated in Figure 8. Here, we first recorded test responses with a standard micropipette filled with saline (Figure 8A). This electrode was then exchanged with one filled with KCl. Following the micropipette exchange, the amplitude of the extracellular EPSP was reduced, as would be expected if the KCl-filled micropipette caused local postsynaptic depolarization, which would reduce the driving force for the EPSC (Figure 8B). The KCl-filled micropipette was then exchanged for one filled with CNQX dissolved in 4M KCl. Again as expected, the population EPSP rapidly disappeared due to the CNQX blockade (Figure 8C). After the response had disappeared, high-frequency trains were delivered as above.

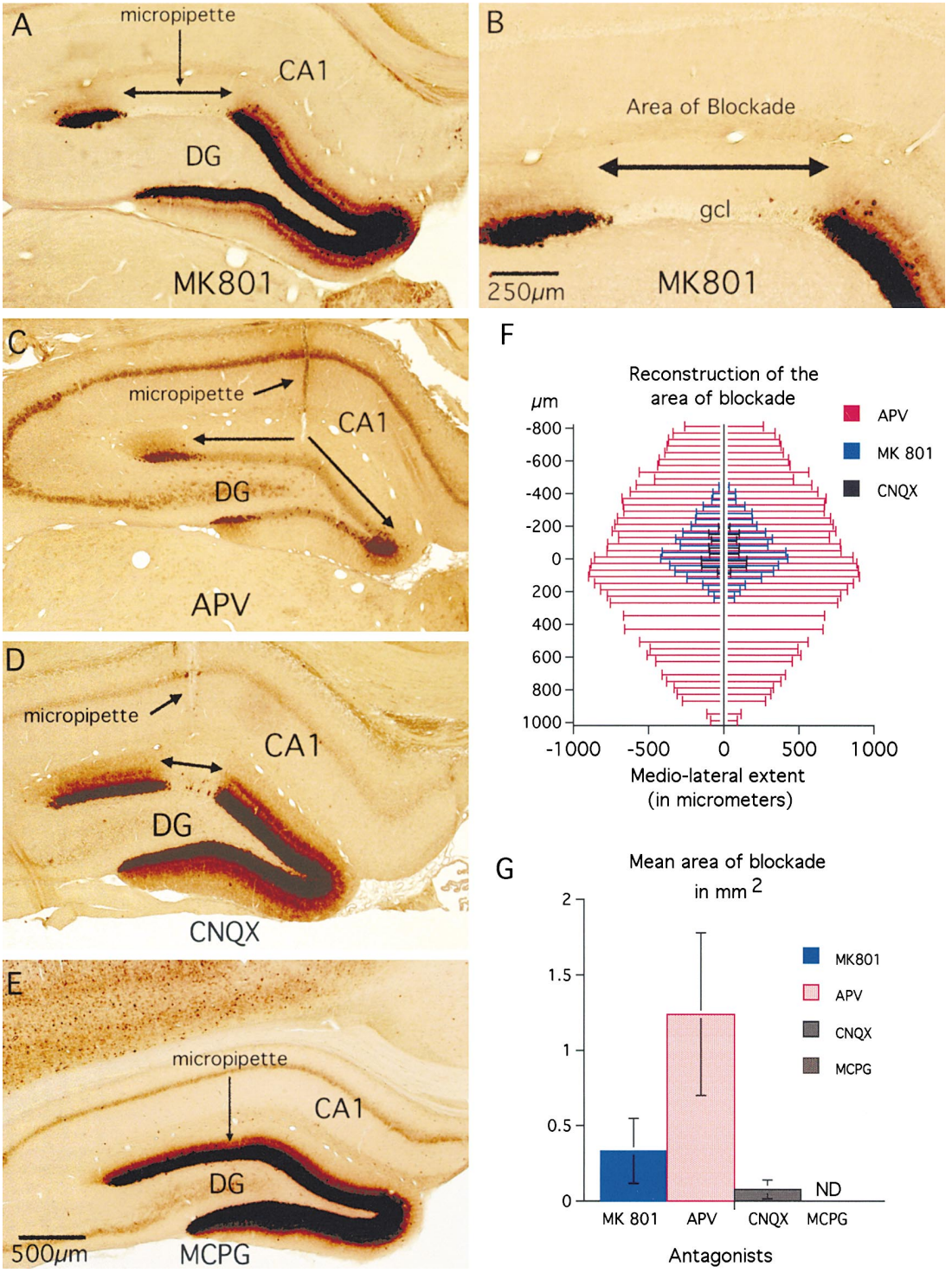

Figure 5. Differential Effects of GluR Antagonists on *Arc* Induction

The photomicrographs illustrate the distribution of *Arc* mRNA in regions surrounding recording micropipettes filled with various GluR antagonists during a period of high-frequency stimulation of the perforant path.

(A and B) The pattern of labeling surrounding a micropipette filled with MK801 (10 mg/ml). Arc induction was completely blocked in an area about 1–2 mm in diameter around the micropipette (the path of the micropipette is indicated by the vertical arrow). B illustrates that in the area of blockade, labeling was present in a small number of granule cells scattered throughout the granule cell layer. This pattern is similar to that seen on the nonstimulated side. In regions distant from the pipette, *Arc* mRNA was strongly induced and selectively localized in the activated lamina.

(C) The pattern of labeling in the area surrounding a micropipette filled with APV (10 mg/ml). Note the extensive blockade of Arc induction throughout most of the dentate gyrus. The micropipette track can be seen in the section (arrow).

With KCl and CNQX in the micropipette, high-frequency stimulation produced a late, slow negativity similar to the late negativity seen in control conditions (compare lower trace, Figure 8D, with Figure 4A). No such negativity was seen with single-pulse stimulation (upper trace, Figure 8D). We interpret this late negativity as reflecting NMDA-receptor activation because the negativity was not seen in experiments in which CNQX was dissolved in saline (Figure 8E). Also, a systemic injection of MK801 (1 mg/kg) given at the end of the 2 hr stimulation period reduced the amplitude of the late slow negative response substantially (data not shown). Thus, the KCl/CNQX combination appears to create a situation in which NMDA receptors can be activated under conditions of AMPA-receptor blockade.

If current flow through the NMDA receptor is sufficient for Arc induction and targeting, then there should be no blockade in the experiments involving CNQX in KCl. This was the case in four of seven experiments (one example is illustrated in Figure 8F). In these four cases, there was no detectable area of blockade of Arc induction around the micropipettes, although the band of labeling in the molecular layer did appear somewhat more blurry than normal. In three experiments, a very small area of blockade was seen. These results demonstrate that induction and localization *can* occur in the presence of AMPA-receptor blockade as long as conditions are such as to allow current flow through the NMDA receptor.

Discussion

Studies of the trafficking of *Arc* mRNA within neurons have revealed highly developed mechanisms for mRNA transport and localization. These studies are possible because Arc is expressed as an immediate early gene. Following an adequate stimulus, the synthesis, intracellular transport, synapse-specific targeting, and life history of the *Arc* transcript can be studied in a way that is not possible with mRNAs that are expressed constitutively. Previous studies have demonstrated that Arc induction depends on NMDA receptor activation (Lyford et al., 1995), that the newly synthesized Arc transcript is rapidly delivered into dendrites based on a targeting signal in the mRNA sequence (Wallace et al., 1998), and that the mRNA localizes selectively at recently-active synapses (Steward et al., 1998). On the basis of these data, we postulated that the localization was mediated by some "address marker" generated as a consequence of synaptic activation. The present results indicate that this address marker is created through NMDA-receptor activation (Figure 9). Hence, both the transcription of *Arc* mRNA in the nucleus and the targeting of the newly synthesized transcript to active synapses are mediated by signal-transduction cascades that are triggered by NMDA-receptor activation. It is certainly an interesting coincidence that these induction mechanisms are shared by LTP.

Localization Requires NMDA Receptor Activation, Not Local Current Flux

High-frequency stimulation activates all types of glutamate receptors, and also causes a massive local current flux in the activated-dendritic domain. In principal, targeting of *Arc* mRNA to activated-dendritic domains could be triggered either by the activation of particular receptors or by the current flux (i.e., an intracellular electrophoresis-like process). NMDA-receptor antagonists did not diminish the fast EPSPs generated by AMPA receptors or the postsynaptic discharge induced by the high-frequency stimulation. Nevertheless, both NMDA-receptor antagonists did effectively block induction and localization. Thus, the massive depolarization mediated by AMPA receptors is *not* sufficient to mediate induction and localization.

There is, however, a late current that is blocked by NMDA-receptor antagonists, and we cannot exclude the possibility that this late NMDA receptor-mediated current contributes to localization. It does not seem likely, however, that this small current would be effective whereas the much larger current generated by AMPA-receptor activation would not. In any case, some signaling process generated by NMDA-receptor activation seems to play the key role.

Given the necessity for NMDA-receptor activation, the obvious candidate for the next step in the signaling cascade is Ca^{2+} flux through the NMDA receptor. Ca^{2+} flux through the NMDA receptor certainly activates a number of kinases, and one of these could in turn activate a docking mechanism through phosphorylation. The present data define one essential criterion for the signaling mechanism. The key molecular modification that mediates localization should itself occur selectively in the activated lamina. It will now be of considerable interest to search for Ca^{2+} mediated molecular alterations that occur selectively in the activated lamina.

The Enabling Role of AMPA Receptors

Blockade of fast synaptic transmission by AMPA-receptor antagonists should also block current flow through the NMDA receptor, because current flow through the NMDA receptor occurs only when the cell is sufficiently depolarized. This occurs during high-frequency stimulation because of AMPA-receptor activation. Thus, it was not surprising that AMPA-receptor antagonists also

(D) The pattern of labeling in the area surrounding a micropipette filled with CNQX (10 mg/ml). Note the small area of blockade of Arc induction surrounding the micropipette track.

(E) The pattern of labeling in the area surrounding a micropipette filled with MCPG (this is a section near the micropipette; the section containing the micropipette track was lost during histological processing). Note that there was no detectable blockade of Arc induction. Abbreviations are as for Figure 1.

(F) A reconstruction of the area of blockade produced by APV, MK801, and CNQX. Each horizontal line indicates the extent of blockade in the dorsal blade of an individual section. Gaps indicate missing sections.

(G) The mean area of blockade in the different groups (± SD). ND indicates that there was no detectable area of blockade in cases involving MCPG.

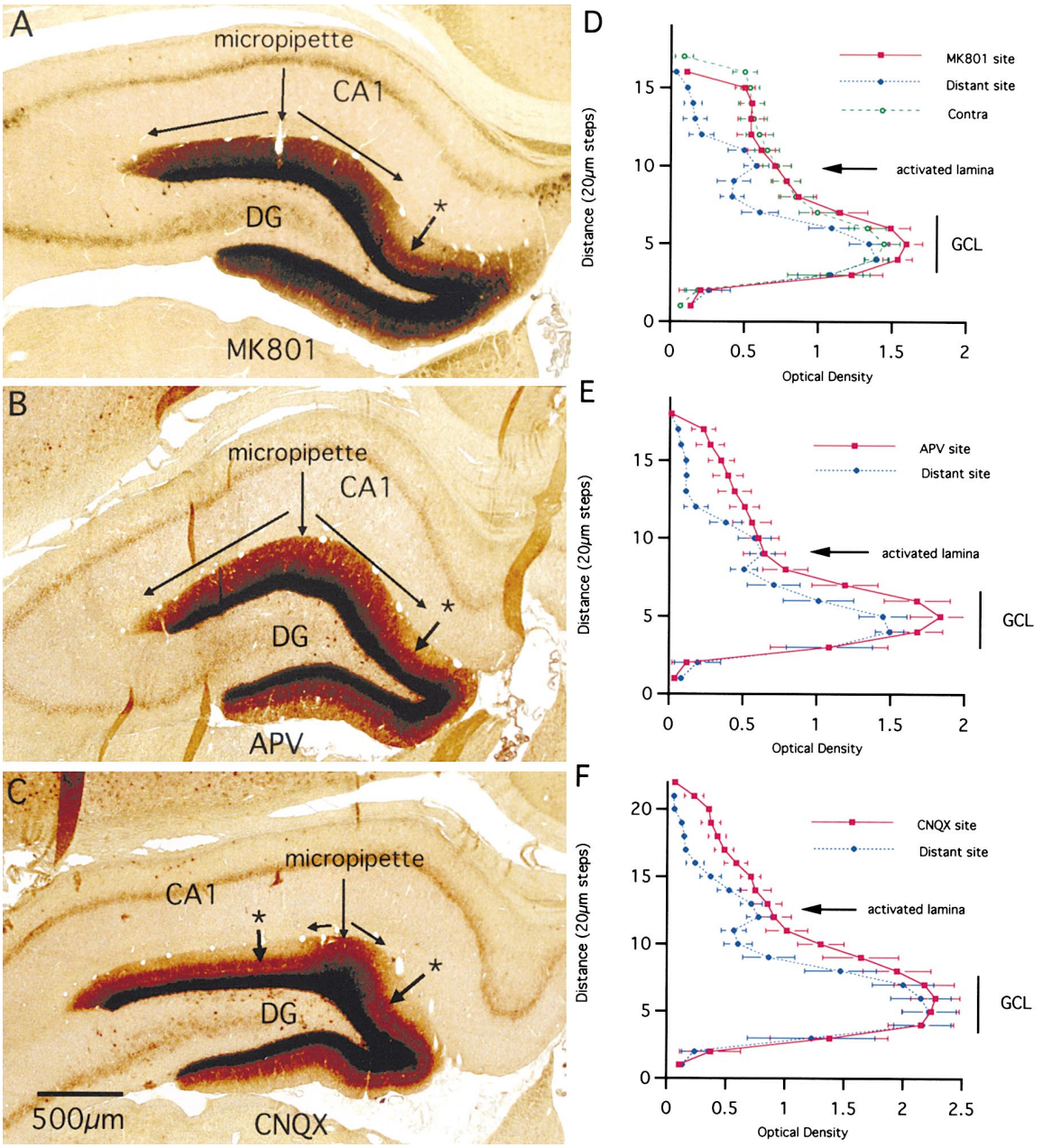

Figure 6. Targeting of Newly Synthesized *Arc* mRNA to Activated Dendritic Domains Is Blocked by NMDA-Receptor Antagonists

The photomicrographs illustrate the distribution of *Arc* mRNA in regions surrounding recording micropipettes filled with various GluR antagonists in animals that had received an ECS and then 2 hr of perforant path stimulation.

(A) The pattern of labeling surrounding a micropipette filled with MK801. Note the absence of the selective band of labeling in the middle molecular layer in an area about 1–2 mm in diameter around the micropipette. In the area of blockade, *Arc* mRNA is uniformly distributed across the molecular layer.

(B) The pattern of labeling surrounding a micropipette filled with APV.

(C) The pattern of labeling surrounding a micropipette filled with CNQX.

(D–F) The graphs illustrate the optical density (OD) of labeling in each situation: area near the antagonist-filled micropipette (APV, MK801, and CNQX sites, respectively); contralateral side that had received ECS only (Contra); and site out of the area of receptor blockade in which the selective band of labeling was still present (Distant site). For APV, the distant site was in a distant section because the area of blockade was so extensive. Abbreviations are as for Figure 1.

blocked Arc induction and targeting in a small region. Nevertheless, the experiments involving KCl demonstrate *can* occur in the presence of AMPA-receptor blockade as long as conditions are such as to allow current flow through the NMDA receptor (for example, as a result of local depolarization). These results indicate that NMDA-receptor activation is both necessary and sufficient for Arc induction and synapse-specific targeting of the mRNA. It must be said, however, that the evidence for sufficiency rests on the KCl/CNQX experi-

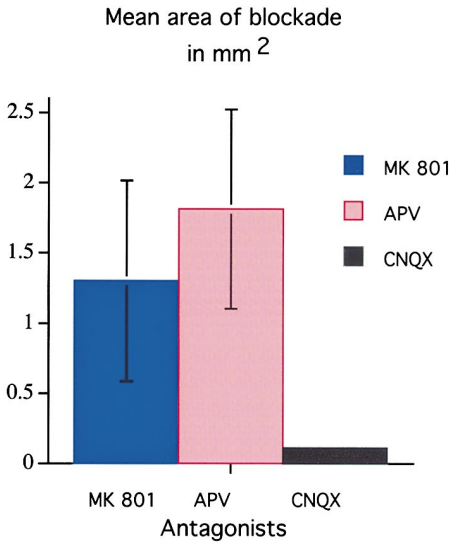

Figure 7. Quantitative Determination of the Area in which mRNA Localization Is Blocked

The bar graph in E illustrates the mean area of blockade across cases (± SD), determined by reconstructing sections as in Figure 5.

ments that are novel, involve two competing pharmacological interventions, and may be subject to unrecognized artifacts.

Given that AMPA-receptor blockade would also block current flow through NMDA receptors, it was surprising that AMPA-receptor antagonists produced such small regions of blockade of induction and targeting. The most likely explanation is that the area of effective blockade produced by CNQX is more limited than for the NMDA-receptor antagonists. This may be due to more limited diffusion in the tissue or to a sharper concentration gradient due to washout or binding.

NMDA-Receptor Mediated Signaling Events

The present results, together with previous findings, establish that the trafficking of *Arc* mRNA involves several distinct steps, and that NMDA-receptor activation is required for at least two of these steps (Figure 9): (1) activity-mediated induction of gene expression (NMDA-receptor dependent); (2) transport of the newly synthesized mRNA from the neuronal cell body into dendrites; and (3) docking of the mRNA at recently activated synapses (NMDA-receptor dependent).

The steps between NMDA-receptor activation and gene induction remain to be established. It could be that there is a discrete signal-transduction cascade that mediates signaling from the active synapses to the nucleus. Alternatively, it is possible that the depolarization produced by NMDA-receptor activation is somehow more effective than the depolarization induced by AMPA receptors and postsynaptic cell discharge in activating Ca^{2+} channels in the soma, which then trigger gene expression in the nucleus. The former seems more likely because the late depolarization resulting from the NMDA receptor is not as great as that induced by AMPA-receptor activation. It remains possible, however, that it is the duration of depolarization that is critical to gene

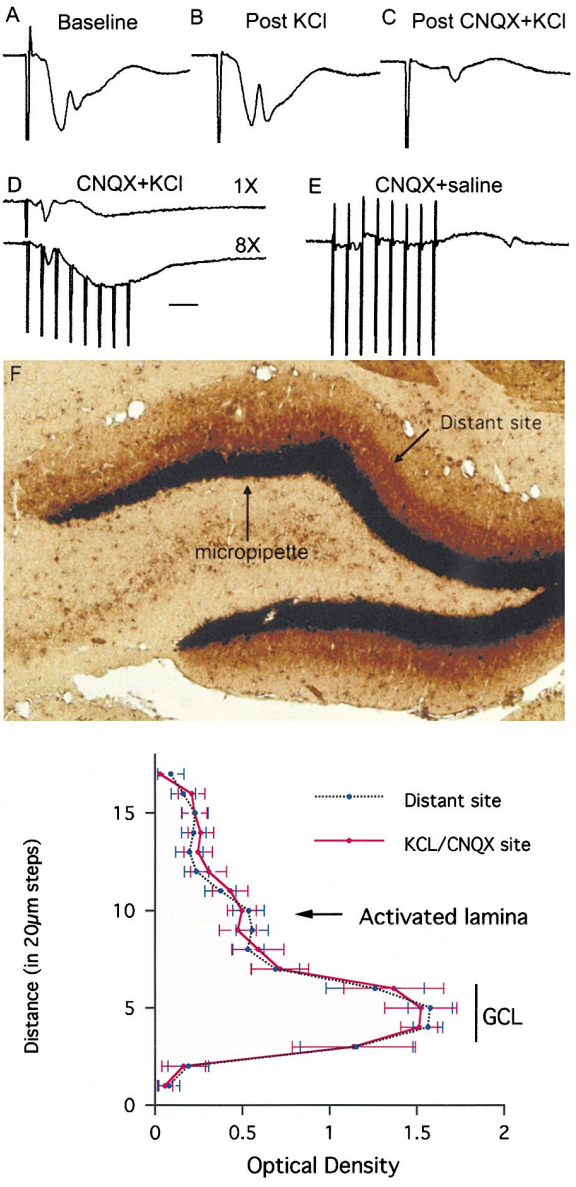

Figure 8. Arc Induction and Targeting with NMDA Receptor Activation under Conditions of AMPA Receptor Blockade

(A) Baseline responses were recorded via a micropipette recording electrode filled with 0.9% saline.

(B) This micropipette was then exchanged with one filled with 4MKCl.

(C) Then, the KCl micropipette was replaced by a pipette filled with CNQX dissolved in 4MKCl, which blocked the fast EPSP.

(D) High-frequency stimulation produced a late, slow negativity, whereas single pulse stimulation did not.

(E) The late negativity was not seen in experiments in which CNQX was dissolved in saline; the response shown is from the same case illustrated in Figure 2B.

(F) One of the cases in which there was no detectable blockade of induction and localization in the area surrounding a KCl/CNQX micropipette after 2 hr of high frequency stimulation. The physiology traces come from a different animal than the in situ hybridization results.

induction. If there is a distinct signal-transduction cascade mediating communication between the activated synapses and the nucleus, it will be of considerable

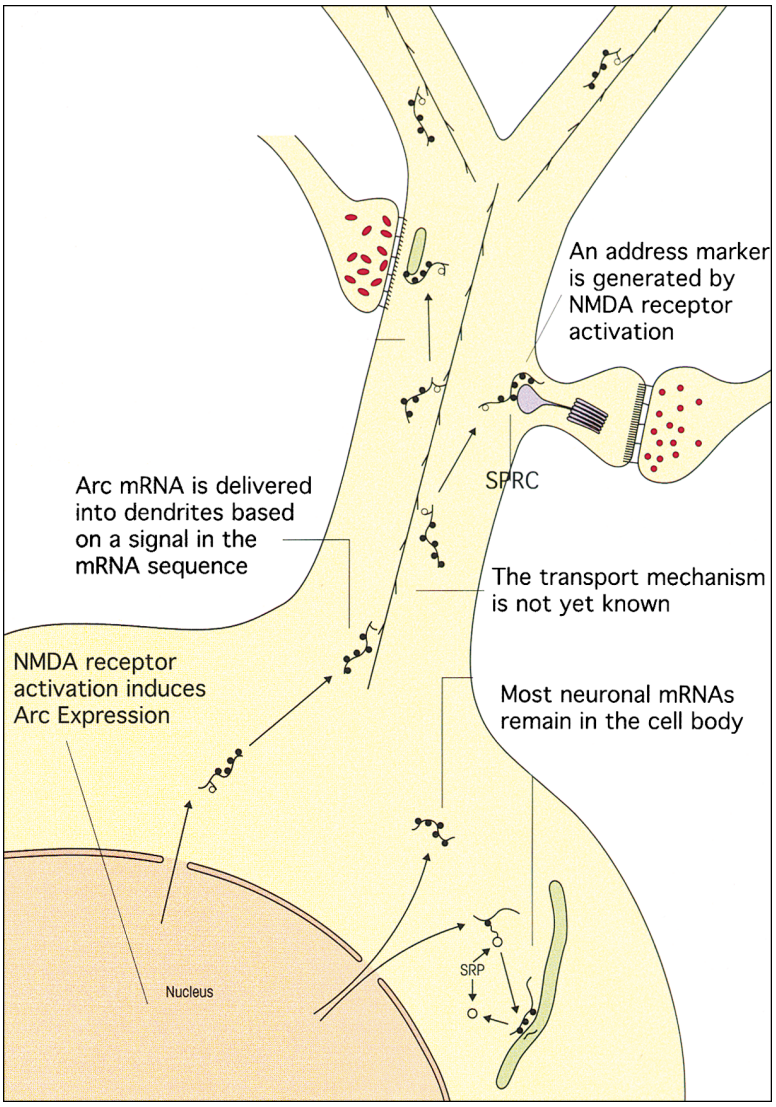

Figure 9. The Steps Involved in Delivering mRNA to Synapses

Modified from Steward, 1993. The trafficking of *Arc* mRNA involves several distinct steps, and NMDA receptors play a key role in at least two of these steps: (1) Arc induction is triggered by NMDA-receptor activation; (2) the mRNA is delivered into dendrites via a mechanism that remains to be defined; and (3) the docking of the mRNA at recently activated synapses is mediated by an address marker generated by prior NMDA-receptor activation. SPRC, synapse-associated polyribosome comoplex.

interest to determine whether the address marker that is critical for mRNA localization is a step along the signal-transduction cascade that also leads to gene induction or is a separate arm of the NMDAR-initiated signaling cascade.

A Link between Activity-Dependent Targeting and mRNA Degradation?

In the experiments involving ECS and subsequent synaptic stimulation, the overall level of labeling for *Arc* mRNA in the dendritic lamina was lower on the side of the synaptic stimulation than on the contralateral side on which Arc had been induced by ECS alone. This suggests that in addition to causing mRNA localization, prolonged synaptic activation also enhances mRNA degradation. In principal, enhanced degradation could be linked to the targeting of the mRNA to the activated dendritic domain. Alternatively, the depletion could be an independent process generated throughout the dendrite as a consequence of the intense depolarization and/or postsynaptic firing caused by the high-frequency stimulation.

The results of NMDA-receptor blockade provide an important clue that distinguishes between these possibilities. Specifically, in the area of blockade, high-frequency stimulation still produces strong synaptic depolarization via AMPA receptors, and also massive postsynaptic discharge, but this dendritic depolarization and postsynaptic firing is not sufficient to cause depletion. This suggests that the depletion is not due to a depolarization-induced enhancement of mRNA degradation but instead is due to some process that is triggered by NMDA receptor activation.

One possible explanation of the decreases in *Arc* mRNA with synaptic activation is that depletion is the end result of three processes: (1) the redistribution of the mRNA inactive to activated laminae and binding at active synapses; (2) localization and/or activity-dependent enhancement of translation; and (3) a translation-dependent enhancement of mRNA degradation. Two lines of circumstantial evidence support this possibility.

First, global inhibition of protein synthesis with cycloheximide following Arc induction by an ECS causes large increases in *Arc* mRNA abundance (Wallace et al., 1998). Second, when protein synthesis is inhibited locally by puromycin during perforant path stimulation, the depletion of *Arc* mRNA is less evident (Steward et al., 1998). Both of these findings suggest translation-dependent mRNA degradation. Although this three-step scenario is consistent with the data, we cannot exclude the possibility that the depletion in the nonactivated dendritic domains is due to some other effect of NMDA-receptor activation.

mRNA Targeting Provides a Potential Mechanism for Enduring Forms of Synapse-Specific Plasticity

Long-lasting forms of activity-dependent synaptic modification (LTP for example) require gene expression and the synthesis of new protein (Frey and Morris, 1997; Kang and Schumann, 1996; Martin et al., 1997; Nguyen and Kandel, 1996). The characteristics of enduring forms of synaptic modification imply that the mechanism involves (1) a signal transduction event at the activated synapses that marks them for subsequent modification; (2) a signaling cascade that modulates gene expression in the nucleus; (3) the synthesis of particular gene products that are necessary for bringing about the synaptic modifications; and (4) the delivery of these gene products to the individual synapses that are to be modified. All of these events must be coordinated in such a way that modifications occur selectively in those synapses that experienced the appropriate patterns of activity.

Studies of Arc have revealed the existence of neuronal mechanisms that could accomplish all of these tasks. Synaptic activity triggers Arc expression; the newly synthesized gene transcripts are delivered selectively to active synapses that have produced the appropriate address marker for mRNA localization, and Arc protein is then made locally near the previously activated synapses. The present study reveals that gene induction, the generation of the address marker at active synapses, and the induction of LTP share a common triggering mechanism (NMDA-receptor activation).

Whether there is an additional targeting step involving the protein itself remains to be established. Indeed, if Arc protein is synthesized at polyribosomes beneath the synaptic membrane specialization, some additional targeting to the synaptic site might be required to assure synapse specificity. If there is such a step, it could well involve the "synaptic tagging" process that has been inferred from physiological studies (Frey and Morris, 1997). Although we use the term "address marker" to distinguish the signals for mRNA localization from the process of synaptic tagging that has previously been described, the two may well be mediated by the same signals.

The pattern of stimulation used to induce *Arc*-mRNA localization is the one that is typically used to induce LTP in the dentate gyrus, and is preferred because this kind of activity simulates patterns of spike trains seen in cortical neurons (for a discussion, see Bliss and Lynch, 1988). It remains to be established whether Arc protein actually plays a role in activity-dependent synaptic modifications, or is instead only a remarkably striking molecular indicator of a general mechanism that neurons possess for targeting mRNAs and proteins to synapses.

Experimental Procedures

Neurophysiological Techniques

Adult male Sprague-Dawley rats were anesthetized by intraperitoneal injection of 20% urethane (500 mg/kg body weight). Supplemental injections of urethane were given approximately every 10 min until the animal was completely unresponsive to tail pinch. The animal was then positioned in a stereotaxic apparatus, a craniotomy was performed, and stimulating and recording electrodes were positioned stereotaxically so as to selectively activate medial peforant path projections while recording in the dentate gyrus, as described in Levy and Steward (1979) and Steward and colleagues (1990). The stimulating electrode (an insulated tungsten microelectrode) was positioned at 4.0 mm lateral to the midline and 1.0 mm anterior to the transverse sinus. The depth of the stimulating electrode was adjusted so as to obtain a maximal evoked response in the dentate gyrus at minimal stimulus intensity. The optimal depth was usually 3–4 mm beneath the cortical surface. Recording electrodes were glass micropipettes filled with 0.9% saline or with various pharmacological agents, as described below. These were lowered into the brain at 3.5 mm posterior to bregma and 1.5–2.0 mm lateral to the midline.

Stimulation Paradigm

During the positioning of the recording electrodes, the micropipette was temporarily positioned in the cell body layer, and stimulus intensity was set so as to evoke an approximately 1–3 mV population spike. Then the micropipette was carefully positioned in the molecular layer of the dorsal blade of the dentate gyrus to record the negative-going population EPSP. Single test pulses were then delivered at a rate of 1/10 s for 5–10 min so as to determine baseline response amplitude. Then the saline-filled electrodes were exchanged with other micropipettes filled either with saline (control exchanges) or the various glutamate receptor antagonists. After the micropipette exchange, test responses were collected for 10–15 min to assess the effects of the antagonists. Then three bouts of high frequency stimulation (ten trains of eight pulses at 400 Hz) were delivered at a rate of 1/10 s. Between each bout of ten trains, ten test responses were collected to determine the extent of synaptic potentiation. After the third bout, high-frequency trains were delivered at a rate of 1/10 s for 15 min–2 hr. At the end of the period of high frequency stimulation, animals received an anesthetic overdose and were perfused for in situ hybridization.

Electroconvulsive seizures (ECS) were induced by delivering AC current (60 Hz, 40 mA for 0.5 s) via ear clip electrodes as described in Wallace et al. (1998). Anesthesia was induced 5 min later, and animals were prepared for neurophysiological recording as described above. High-frequency stimulation commenced 30–45 min after the ECS.

Local Delivery of Pharmacological Agents

To block glutamate receptors (GluR), recording micropipette electrodes were prepared by breaking back the tips of the electrodes so that the internal diameter of the tip was approximately 30 μm. The micropipettes were filled with a 0.9% saline solution containing MK801, APV, CNQX (the disodium salt), DNQX, or MCPG (all at a concentration of 10 mg/ml of 0.9% saline). MK801 was obtained from Tocris Cookson (Ballwin, MO). The other antagonists were obtained from Research Biochemicals (Natick, MA). CNQX and DNQX were solubilized by briefly heating the solution to about 90°C, but there was some re-crystallization as the solutions cooled. Thus, the effective concentration of CNQX and DNQX was less than the nominal concentration.

In Situ Hybridization and Immunocytochemistry

At the termination of the neurophysiological experiment, rats received a lethal dose of anesthetic (100 mg/kg of Nembutal given i.p.). When deeply anesthetized, the animals were perfused with 4% paraformaldehyde. The brains were removed and stored in fixative

for 1–5 days. One set of brains was sectioned using a vibratome, and sections were collected and stored in phosphate buffer (pH 7.4). Sections were mounted on polylysine-coated microscope slides, and were then hybridized with digoxygenin-labeled cRNA probes as described in Wallace et al. (1998). Details regarding the cRNA probes used for *Arc* have been described previously (Wallace et al., 1998).

Another group of animals was prepared specifically to allow a reconstruction of the area of blockade produced by the various antagonists (for numbers of animals in each group, see Results). The animals were perfused as described above, the brains were stored overnight in fixative, and were then cryoprotected by overnight storage in 30% sucrose. Brains were then frozen by immersion in liquid nitrogen and sectioned on a cryostat. Serial cryostat sections were collected and stored at −80°C until they were prepared for in situ hybridization.

Quantitative Analyses

Serial-Section Reconstruction of the Area of Blockade Produced by GluR Antagonists

To determine the total area of blockade produced by the antagonists, we used the cases in which serial cryostat sections had been collected, preparing alternate sections for in situ hybridization. We then measured the linear extent of blockade in the dorsal blade of each individual section using the "length" function of an M4 Microcomputer Imaging Device (MCID) (Imaging Research, St. Catharines, ON, Canada). The area of blockade in each section was thus represented by a line of a particular length. The total area of blockade was then reconstructed by stacking the sections, with intersection spacing scaled for section thickness (20 μm, see Figure 5F). We then measured the total area of the stack using the "area" function of the MCID system. This value was then averaged across cases.

We focused on the dorsal blade of the dentate gyrus for the area measurements because the electrode tip was centered in this blade. Assuming that the tip represents the center of the area of diffusion, the linear distance along the granule cell layer of the dorsal leaf would correspond approximately to the diameter of the affected area. We did not measure areas of blockade that extended into the ventral blade (see Figure 5C), because this would not be along the plane that represented the diameter of the affected area.

Densitometric Measurement of Labeling Intensity

For quantitative assessment of labeling, optical density (OD) measurements were taken across the granule cell layer and molecular layer using an M4 Microcomputer Imaging Device (MCID), (Imaging Research, St. Catharines, ON, Canada). Digital images of an area of the supra-pyramidal blade of the dentate gyrus were collected at 400×. The light intensity was adjusted so that areas exhibiting background levels of labeling (the hilus contralateral to the side of the stimulation) were just above threshold whereas areas exhibiting maximal levels of labeling (the granule cell layer ipsilateral to the stimulation) were within the measuring range. Then, a series of OD measurements were taken across the granule cell layer and molecular layers using a 20 μm × 20 μm measuring frame. A row of five separate measurements was taken at 20 μm steps across the granule cell layer and molecular layer, and the OD values at each step were averaged. The values in the graphs illustrate the mean and standard deviation of the five measurements.

Acknowledgments

Thanks to Kelli Sharp and Jamie Zaffis for technical assistance. This work was supported by NIH grants NS12333 (O. S.) and MH53603 (P. F. W.).

Received May 18, 2000; revised February 2, 2001.

References

Bliss, T.V.P., and Lynch, M.A. (1988). Long-term potentiation of synaptic transmission in the hippocampus: properties and mechanisms. In Long-Term Potentiation: From Biophysics to Behavior, P.W. Landfield and S.A. Deadwyler, eds. (New York, Alan R. Liss), pp. 3–72.

Frey, U., and Morris, R.G.M. (1997). Synaptic tagging and long-term potentiation. Nature *385*, 533–536.

Kang, H., and Schumann, E.M. (1996). A requirement for local protein synthesis in neurotrophin-induced hippocampal synaptic plasticity. Science *273*, 1402–1406.

Levy, W.B., and Steward, O. (1979). Synapses as associative memory elements in the hippocampal formation. Brain Res. *175*, 233–245.

Link, W., Konietzko, G., Kauselmann, G., Krug, M., Schwanke, B., Frey, U., and Kuhl, K. (1995). Somatodendritic expression of an immediate early gene is regulated by synaptic activity. Proc. Natl. Acad. Sci. USA *92*, 5734–5738.

Lyford, G., Yamagata, K., Kaufmann, W., Barnes, C., Sanders, L., Copeland, N., Gilbert, D., Jenkins, N., Lanahan, A., and Worley, P. (1995). Arc, a growth factor and activity-regulated gene, encodes a novel cytoskeleton-associated protein that is enriched in neuronal dendrites. Neuron *14*, 433–445.

Martin, K.C., Casadio, A., Zhu, H., E, Y., Rose, J.C., Chen, M., Bailey, C.H., and Kandel, E.R. (1997). Synapse-specific, long-term facilitation of aplysia sensory to motor synapses: A function for local protein synthesis in memory storage. Cell *91*, 927–938.

Nguyen, P.V., and Kandel, E.R. (1996). A macromolecular synthesis-dependent late phase of long-term potentiation requiring cAMP in the medial perforant pathway of rat hippocampal slices. J. Neurosci. *16*, 3189–3198.

Steward, O. (1993). Synapse growth as a mechanism for activity-dependent synaptic modification. In Seventh Novo Nordisk Foundation Symposium: Memory and Concepts: Basic and Clinical Aspects, P. Andersen, O. Hvalby, O. Paulsen, and B. Hokfelt, eds. (Amsterdam: Elsevier), pp. 281–301.

Steward, O., Tomasulo, R., and Levy, W.B. (1990). Blockade of inhibition in a pathway with dual excitatory and inhibitory action unmasks a capability for LTP that is otherwise not expressed. Brain Res. *516,* 292–300.

Steward, O., Wallace, C.S., Lyford, G.L., and Worley, P.F. (1998). Synaptic activation causes the mRNA for the IEG Arc to localize selectively near activated postsynaptic sites on dendrites. Neuron *21*, 741–751.

Wallace, C.S., Lyford, G.L., Worley, P.F., and Steward, O. (1998). Differential intracellular sorting of immediate early gene mRNAs depends on signals in the mRNA sequence. J. Neurosci. *18*, 26–35.